ELSEVIER

Journal of Photochemistry and Photobiology A: Chemistry 130 (2000) 49–56

Journal of Photochemistry and Photobiology A:Chemistry

www.elsevier.nl/locate/jphotochem

Photocurrent generated on a carotenoid-sensitized TiO_2 nanocrystalline mesoporous electrode

Frank G. Gao [a], Allen J. Bard [a], Lowell D. Kispert [b,*]

[a] Department of Chemistry & Biochemistry, University of Texas, Austin, TX 78712, USA
[b] Department of Chemistry, University of Alabama, Tuscaloosa, AL 35487-0336, USA

Received 10 June 1999; received in revised form 7 September 1999; accepted 13 September 1999

Abstract

Photocurrent was observed upon monochromatic illumination of an ITO electrode coated with a TiO_2 nanocrystalline mesoporous membrane with carotenoid 8′-apo-β-caroten-8′-oic acid (ACOA) deposited as a sensitizer (illuminated area 0.25 cm^2) and immersed in an aqueous 10 mM hydroquinone (H_2Q), 0.1 M NaH_2PO_4 solution (pH = 7.4) purged with argon, using a platinum flag counter electrode (area 3.3 cm^2) and a SCE reference electrode. The carotenoid-sensitized short-circuit photocurrent reached 4.6 μA/cm^2 upon a 40 μW/cm^2 incident light beam at 426 nm, with an IPCE (%, incident monochromatic photon-to-photocurrent conversion efficiency) as high as 34%. The short-circuit photocurrent was stable during 1 h of continuous illumination with only a 10% decrease. An open-circuit voltage of 0.15 V was obtained (upon 426 nm, 40 μW/cm^2 illumination) which remained at a constant value for hours. The observed open-circuit voltage is close to the theoretical value (0.22 V) expected in such a system. The action spectrum resembled the absorption spectrum of ACOA bound on the TiO_2 membrane with a maximum near 426 nm. No decay of the ACOA on the TiO_2 surface was observed after 12 h, presumably because of rapid regeneration of ACOA from $ACOA^{\bullet +}$ at the surface by electron transfer from H_2Q. ©2000 Elsevier Science S.A. All rights reserved.

Keywords: Photocurrent; Indium tin oxide; 8′-apo-β-caroten-8′-oic acid; TiO_2 mesoporous electrode

1. Introduction

Although carotenoids in solution are generally not photochemically reactive because the life time of the S_1 excited state of carotenoid pigments is usually very short (10–50 ps), carotenoids can undergo photochemical reactions such as unimolecular isomerization [1,2], quenching of triplet or singlet states of other molecules through energy transfer [3], intramolecular charge-transfer [4], charge separation in synthetic molecular dyads and triads [5–7], and photoinduced electron-transfer to solvent molecules [8,9]. Electrons can be transferred from excited states of a carotenoid to the conduction band of semiconductor particles and cause enhanced photodegradation and photoisomerization of the carotenoids depending on the properties of both carotenoid and semiconductor [10]. Further, carotenoids can serve as light-harvesting accessory pigments in photosynthetic plants by transferring the singlet excitation energy to chlorophyll a (Chl a). They also act as ‘triplet valves’ to harmlessly dissipate the energy of Chl triplets and are scavengers of singlet oxygen which can destroy Chl [11]. In addition, the highly conjugated carotenoids can function as short molecular wires that mediate electron transfer in donor–acceptor complexes and membranes [12,13]. Photoconduction properties of carotenoids were systematically studied, and effective production of charge carriers by excitation of carotenoid absorption bands was observed [14–16]. These properties, together with their characteristic light absorption in the range of 380–520 nm and molar extinction coefficients larger than 10^5, make certain carotenoids potential sensitizer materials in solar photovoltaic cells and other artificial photochemical devices. Sandwich cells of the type (Al|Chl a|mixture of Chl a and canthaxanthin|Chl a|Ag) have been used in measurements of photovoltaic currents [17]. A photocurrent, generated by irradiation with light that is in the canthaxanthin absorption region, was attributed to energy transfer from canthaxanthin to Chl a. The long conjugated chain of canthaxanthin may behave as a photoconductor and serve to reduce the internal resistance of the cells [17]. Indium tin oxide (ITO) electrodes coated with LB (Langmuir–Blodgett) films of 7′-apo-7′-(4-carboxyphenyl)-β-carotene and immersed in

---

[*] Corresponding author. Tel.: +1-205-348-8436; fax: +1-205-348-9104
E-mail address: lkispert@bama.ua.edu (L.D. Kispert)

1010-6030/00/$ – see front matter ©2000 Elsevier Science S.A. All rights reserved.
PII: S1010-6030(99)00193-8

an electrolyte solution also containing benzoquinone (Q) or hydroquinone (H_2Q) have been shown to be photoactive [18]. An organized assembly of the carotenoid pigments in contact with the ITO electrode was formed, so that electron transfer between the pigment and the electrode can effectively compete with the decay of the carotenoid excited state. The resulting photocurrent ($\sim$2 nA/cm^2) and action spectra measurements implicated the excited carotenoid pigment as the photoactive species in the electron transfer process. However, although all these approaches using carotenoids did show generation of photocurrents upon illumination, the incident photon-to-electron conversion efficiency (IPCE) is very low (<0.4%).

During the past decade, the utilization of semiconductors as catalysts in solar energy conversion, photochemical transformations of organic and inorganic compounds, and photodegradation of organic pollutants has seen a tremendous growth [19]. Among the many semiconductors used in past and present research in photocatalysis, titanium dioxide (TiO_2) features prominently. Recently application of dye-sensitized semiconductor electrodes to a new type of photovoltaic cell, the dye-sensitized TiO_2 nanocrystalline solar cell or Graetzel cell [20], has stimulated much interest [21,22]. Photosensitization, which is achieved by adsorption of dye molecules on the surface of a large-bandgap semiconductor, such as TiO_2, and injection of an electron into its conduction band upon visible excitation, provides an efficient wet chemical method for converting sunlight into chemical or electrical energy, and overcomes the limitation of non-coated metal oxide semiconductors that are only photoactive when exposed to UV light. Although many organic dyes, e.g., Ru complexes [23,24], erythrosin B [25], eosin [26], phthalocyanines [27], oxazines [28], and squaraine [29], have been studied for sensitization of large-bandgap semiconductors. Development of new semiconductor sensitizers which produce higher conversion efficiency and low cost solar photovoltaic dye cells is a long-term task.

Studies indicate that electron transfer from the electronically excited photosensitizer *cis*-$(H_2O)_2$bis(2,2′-bipyridyl-4,4′-dicarboxylate) ruthenium (II), adsorbed on the surface of TiO_2 nanocrystals, to TiO_2 is a very fast process (<7 ps) [20]. This may imply that, given the lifetime (10–50 ps) of the S_1 excited state of carotenoid (Car*), the electron transfer from Car* to TiO_2 could also occur. In a recent study [30], photovoltaic currents ($\sim$10 nA/cm^2) were indeed observed upon irradiating an ITO electrode spin-coated with a mixture of TiO_2 nanoparticles, polyvinyl carbazole, and carotenoid (canthaxanthin or β-carotene) and immersed in an aqueous KCl solution containing hydroquinone. However, the IPCE is still very low, and the possibility of using carotenoids in artificial photochemical devices is vague.

To overcome the kinetic limitation of efficient photoinjection and movement of electrons imposed by the short singlet excited state lifetime, carotenoids should be incorporated into a structure in which ultrafast photoinduced electron transfer can occur and therefore increase the cell efficiency. One strategy to accomplish this is to directly coordinate a carotenoid substituted with a terminal carboxylate group to the TiO_2 surface via formation of covalent bonds.

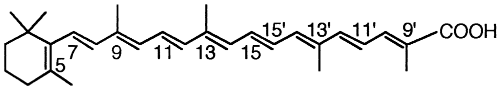

Scheme 1. Structure of 8′-apo-β-caroten-8′-oic acid (ACOA).

In this study, ITO electrodes coated with a TiO_2 nanoparticle membrane and carotenoid 8′-apo-β-caroten-8′-oic acid (ACOA) deposited as a sensitizer were investigated for generation of photocurrents in a photochemical cell. It turned out that such a cell shows a very high quantum efficiency for incident photon-to-electron conversion (IPCE = 34%), with photocurrent and photovoltage stable for hours. This finding is of fundamental interest in both photochemistry and carotenoid chemistry; it changes the earlier view of carotenoids and converts it to a potential new sensitizer.

2. Experimental

2.1. Materials

All-*trans*-8′-apo-β-caroten-8′-oic acid (ACOA) was synthesized by Dr. Elli Hand [31]. Its structure is shown in Scheme 1. Sodium phosphate monobasic monohydrate ($NaH_2PO_4 \cdot H_2O$), sodium hydroxide, and nitric acid (69.0–71.0%) (all GR grade) were purchased from EM Science. Tetra-*n*-butylammonium hexafluorophosphate (TBAHFP) of polarographic grade was purchased from Fluka. Hydroquinone (99+%), anhydrous dichloromethane (99+%), polyethylene glycol (PEG, M-20,000), and titanium (IV) isopropoxide (97%, $Ti[OCH(CH_3)_2]_4$) were purchased from Aldrich. Absolute ethanol was purchased from McCormick Distilling Co., Weston, Missouri. Highly purified water (Millipore Milli-Q, 18 MΩ cm) was used to prepare electrolyte solutions. Transparent glass plates (1.6 cm × 4.2 cm) coated with InO_2/SnO_2 (ITO, 100 Ω per square) was from Delta Technologies. ITO plates were boiled in water containing 5% detergent for 1 h, rinsed thoroughly with water, soaked in pure water and ethanol, each for 10 h, dried at 90°C for 5 h, and then stored in a desiccator over drierite at room temperature for later use.

2.2. Preparation of TiO_2 nanocrystalline colloidal solution

TiO_2 nanocrystalline colloidal solution was prepared by hydrolysis of titanium (IV) isopropoxide according to the procedure described in [32,33]. In brief, under a stream of dry nitrogen, 125 ml of $Ti[OCH(CH_3)_2]_4$ was added to a 250 ml dropping funnel containing 20 ml ethanol and mixed well. The mixture was slowly ($\sim$10 min) dropped into a 1 l flask containing 750 ml of vigorously stirred pure water. A white precipitate was formed during the hydrolysis. Within

10 min, 5.3 ml of concentrated nitric acid was added to the hydrolysis mixture, still stirring vigorously. The mixture was then stirred for 8 h at 80°C to give a stable transparent TiO_2 colloidal solution. The size of the colloidal anatase TiO_2 particles obtained by this procedure was ca. 8 nm. The resulting solution was stored in the dark at room temperature for later use.

2.3. Preparation of ITO electrode coated with TiO_2 nanocrystalline mesoporous membrane with ACOA deposited as a sensitizer

A 100 ml TiO_2 colloidal solution was concentrated to about 20 ml by evaporation of water under reduced pressure at room temperature. 1.2 g PEG was added and the mixture was stirred to make a viscous TiO_2 dispersion. The TiO_2 dispersion was spin-coated on the ITO surface at 2000 rpm for 40 s and then calcined at 450°C for 30 min, 150°C for 5 min, and then transferred to a desiccator over drierite to cool to room temperature. A rigid and transparent TiO_2 nanocrystalline mesoporous membrane was formed by this procedure. The ITO/TiO_2 plate was immersed in an ethanol solution of 0.3 mM ACOA for 4 h in the dark at room temperature, and rinsed three times with ethanol before measurement.

2.4. Photoelectrochemical measurements

Photoelectrochemical measurements of the photocurrent at a fixed electrode potential were carried out using the Bio Analytical Systems BAS-100W electrochemical analyzer. A homemade electrochemical cell consisting of a 12 ml Teflon vessel with a flat quartz glass window used for irradiation of the ITO working electrode surface (illuminated area 0.25 cm^2), was equipped with a saturated calomel electrode (SCE) and a platinum flag (3.25 cm^2) as the reference and counter electrodes, respectively. In measuring the short-circuit photocurrent, the reference was connected to the counter electrode with zero bias applied. An aqueous solution of 10 mM H_2Q and 0.1 M NaH_2PO_4 (pH was adjusted to 7.4 by NaOH aq. solution) was added to the cell and purged with argon for 20 min; argon was continuously passed over the surface of the solution during the experiments. The open-circuit photovoltage was measured by an x-y recorder (SOLTEC, VP-64235, input impedance 1 MΩ), using its time base function. A 250 W xenon lamp (Oriel) and a monochromator (Oriel) were used as a monochromatic irradiation source in the steady-state measurements. Water contained in a cylindrical glass cell (path length, 13 cm) was used as an IR cut-off filter between the lamp and monochromator. The light intensity at the external surface of the cell, measured with a Newport power meter (Model 818-SL), was between 20–80 μW/cm^2 at 426 nm depending on the adjusted power of the lamp.

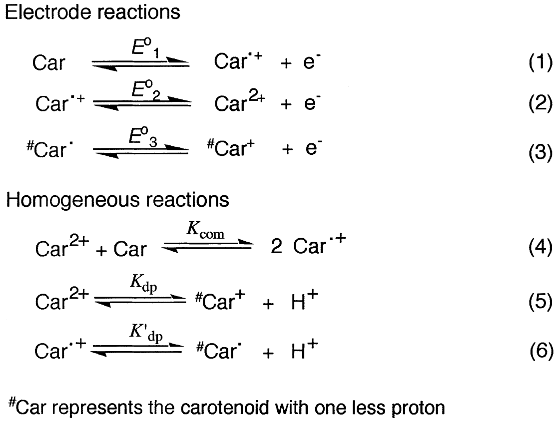

Electrode reactions

$$\mathrm{Car} \xrightleftharpoons{E^{o}_{1}} \mathrm{Car}^{\bullet +} + e^{-} \qquad (1)$$

$$\mathrm{Car}^{\bullet +} \xrightleftharpoons{E^{o}_{2}} \mathrm{Car}^{2+} + e^{-} \qquad (2)$$

$$^{\#}\mathrm{Car}^{\bullet} \xrightleftharpoons{E^{o}_{3}} {}^{\#}\mathrm{Car}^{+} + e^{-} \qquad (3)$$

Homogeneous reactions

$$\mathrm{Car}^{2+} + \mathrm{Car} \xrightleftharpoons{K_{\mathrm{com}}} 2\ \mathrm{Car}^{\bullet +} \qquad (4)$$

$$\mathrm{Car}^{2+} \xrightleftharpoons{K_{\mathrm{dp}}} {}^{\#}\mathrm{Car}^{+} + H^{+} \qquad (5)$$

$$\mathrm{Car}^{\bullet +} \xrightleftharpoons{K'_{\mathrm{dp}}} {}^{\#}\mathrm{Car}^{\bullet} + H^{+} \qquad (6)$$

$^{\#}$Car represents the carotenoid with one less proton

Scheme 2.

2.5. Other measurements

Cyclic voltammetry (CV) of the dichloromethane solution with 2 mM ACOA and 0.1 M TBAHFP was carried out using the BAS-100W electrochemical analyzer. A platinum disk electrode (diameter = 1.6 mm) was used as the working electrode, the auxiliary electrode was a platinum wire, and the reference electrode was a SCE. Optical absorption spectra in the range of 200–900 nm were measured using a Milton Roy Spectronic 3000 diode array UV–VIS spectrophotometer (Milton Roy, San Leandro, CA). A piece of ITO/TiO_2 or ITO/TiO_2/ACOA plate was directly placed in the sample holder using a bare ITO or air as reference. For the measurements of the optical absorption spectrum of 7 μM ACOA dichloromethane solution, quartz cuvettes (1 cm optical path length) were used. An AFM image of a piece of ITO/TiO_2 plate was taken after the plate was calcined and cooled. Images were recorded with a Nanoscope III with an AFM 619E-Z head (Digital Instruments, Santa Barbara, CA) using a SiN tip in the contact mode.

3. Results and discussion

3.1. Cyclic voltammetry and optical absorption spectrum of ACOA

Previous investigations [34–39] of a variety of different carotenoids have established that the electrode and homogeneous reactions shown in Scheme 2 take place during the electrochemical oxidation of most carotenoids at ambient temperatures. Canthaxanthin is one of the most intensively studied; its redox reactions (Eqs. (1)–(3)) can be detected by cyclic voltammetry (CV) in dichloromethane. For canthaxanthin, the CV shows two comparable pairs of peaks in a positive and reversal sweeping cycle. The first oxidation peak corresponds to the one-electron oxidation of the neutral species (Eq. (1)), and the second oxidation peak results from the subsequent one-electron oxidation of the radical cation (Eq. (2)). Two reverse reduction peaks are due to sequen-

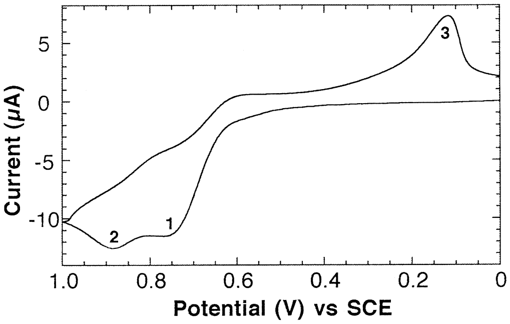

Fig. 1. Cyclic voltammogram of 1 mM ACOA and 0.1 M TBAHFP in dichloromethane solution with a platinum disc electrode. Scan rate 100 mV s^{-1}.

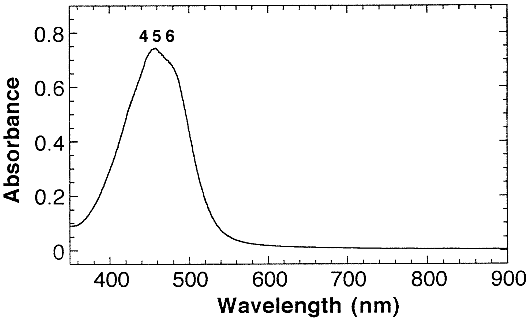

Fig. 2. Optical absorption spectrum of 7 μM ACOA dichloromethane solution, using quartz cuvettes.

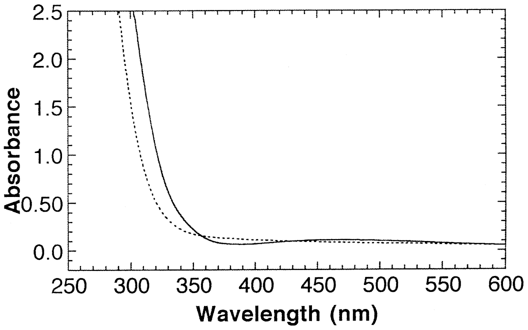

Fig. 3. Optical absorption spectra of an ITO coated with nanocrystalline TiO_2 membrane (solid line) and a bare ITO plate (dotted line), versus air.

tial one-electron reductions of the dication and the radical cation. Another reduction peak at lower potential (~0.2 V) results from the reduction (reverse of Eq. (3)) of the transient intermediate, $^{\#}Car^{+}$, which is formed by loss of a proton from the dication (Eq. (5)); reduction of the deprotonated radical cation (Eq. (6)) also contributes to this peak.

The CV of ACOA obtained in dichloromethane using a platinum disc electrode at room temperature is shown in Fig. 1. In the positive sweep, two peaks (1 and 2) were observed which correspond to two one-electron oxidations. Rapid deprotonation of ACOA radical cations ($ACOA^{\bullet +}$) presumably occurred to form ACOA radicals with one less proton ($^{\#}ACOA^{\bullet}$). $^{\#}ACOA^{\bullet}$ subsequently lost one electron to form $^{\#}ACOA^{+}$, and reduction of $^{\#}ACOA^{+}$ to $^{\#}ACOA^{\bullet}$ near 0.1 V gave peak 3. This mechanism could explain the CV of ACOA showing an intense peak 1 and a weak peak 2. The first half-wave potential of $ACOA/ACOA^{\bullet +}$ couple can be estimated as 0.68 V versus SCE.

A neutral solution of ACOA is orange red in color with an extinction coefficient ($\varepsilon_{\mathrm{mol}}$) of ca. 1×10^5. Fig. 2 shows the optical absorption spectrum of a 7 μM ACOA dichloromethane solution with an absorption maximum at 456 nm.

3.2. Characteristics of mesoporous TiO_2 nanocrystalline membrane

An ITO coated with a thin membrane of nanocrystalline TiO_2 was prepared according to the process described in the experimental section. The TiO_2 membrane is transparent, and there is no absorption above 370 nm as shown by the optical absorption spectrum of an ITO/TiO_2 plate (Fig. 3, solid line), indicating the 'Q particles' characteristic of the TiO_2 particles in the film [40]. One of the predicted properties of 'Q particles' (in the range 5–25 nm) is an increase in E_{gb} and therefore a blue shift in the absorption edge, with decreasing particle size [41]. Fig. 3, dotted line, shows the absorption spectrum of a bare ITO plate, indicating absorption by SnO_2 at shorter wavelength as is expected. AFM images of a variety of ITO/TiO_2 plates showed a highly porous surface structure. As shown in Fig. 4, the membrane consists of holes and mounds interconnected in a three-dimensional network; these large mounds are bonded together by smaller TiO_2 particles. In contrast, the AFM image of a bare ITO plate obtained under the same condition showed a relatively smooth surface.

3.3. Absorption spectrum of ACOA deposited on a ITO/TiO_2 electrode

The optical absorption spectrum of ACOA deposited on a ITO/TiO_2 plate versus a piece of bare ITO, measured in air, is shown in Fig. 5. It exhibits an absorption maximum at 426 nm, indicating that the ACOA molecules have been attached to the TiO_2 surface. Formation of monolayers of ACOA, perhaps ordered, on the TiO_2 particles could account for the 30 nm blue-shift from 456 nm (ACOA in dichloromethane) to 426 nm (ACOA on TiO_2 surface). In addition, interaction of ACOA molecules with TiO_2 particles to form surface complexes might slightly change the electronic state of ACOA molecules, resulting in the change of transitions. Scheme 3 is a representation of ACOA complexes formed with metallic sites in solid TiO_2. By direct coordination of a carotenoid substituted with a terminal carboxylic acid group to the TiO_2 surface, formation of covalent bonds was achieved, although the detailed reaction has not been investigated. Formation of surface complexes via Ti–O covalent bonds between compounds with a terminal carboxilic acid group and TiO_2 has been intensively investigated and confirmed [20,42–44].

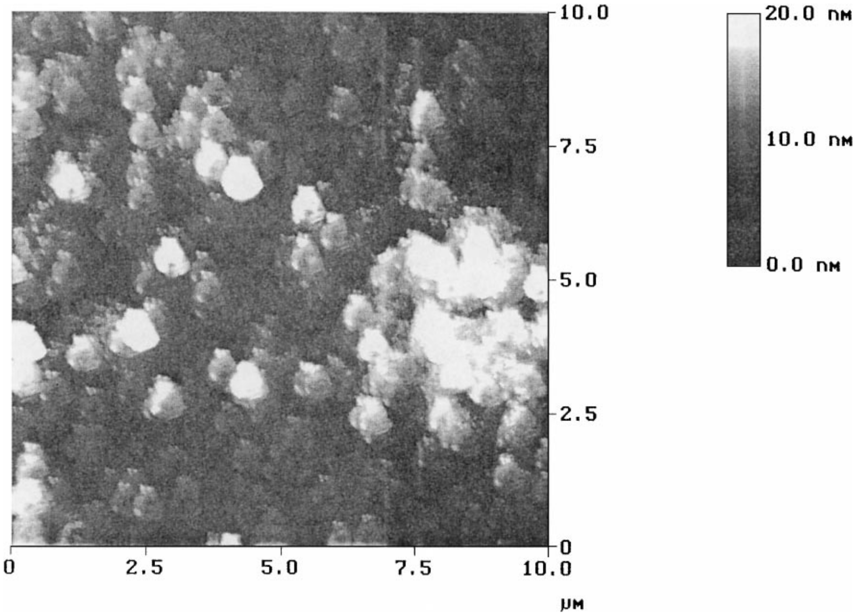

Fig. 4. AFM image of an ITO coated with a nanocrystalline TiO_2 membrane.

3.4. Short-circuit photocurrent and open-circuit photovoltage generation from an ITO/TIO_2 electrode by photosensitization of ACOA in a photoelectrochemical cell, and cell efficiency

Fig. 6 (solid line) shows the short-circuit photocurrent observed upon monochromatic irradiation (426 nm, 40 μW/cm^2) of an ITO/TiO_2/ACOA electrode in a photoelectrochemical cell. Upon illumination, the anodic photocurrent (the anodic current is shown as negative) rose rapidly and reached an approximately steady-state value of 1.2 μA (a photocurrent density of 4.6 μA/cm^2). The photocurrent returned to a low level after illumination was terminated. Under the same conditions, with a bare ITO/TiO_2 plate as working electrode, essentially no photocurrent was detected (Fig. 6, dotted line). Therefore the origin of the photocurrent must be attributed to excitation of ACOA. The photocurrent readout as a function of illumination time is shown in Fig. 7. The photocurrent decreased only 10% during 1 h of continuous illumination.

The incident monochromatic photon-to-photocurrent conversion efficiency (IPCE), defined as the number of electrons produced in the external circuit divided by the number of incident photons, can be calculated according to the following equation [45]:

$$\mathrm{IPCE}\,(\%) = 100 \times \frac{1240 i_{\mathrm{sc}}}{I_{\mathrm{inc}}\lambda} \tag{7}$$

where i_{sc} is the short-circuit photocurrent (A/cm^2). I_{inc} is the incident light intensity and λ is the excitation wavelength (nm).

Evaluation of the data from Fig. 6 gave an IPCE of 34% for the short-circuit photocurrent sensitized by ACOA deposited on an ITO/TiO_2 electrode upon illumination by monochromatic light at 426 nm. Similar experiments under varied incident light intensities from 20 to 80 μW/cm^2 were repeated many times and IPCE values around 35% were consistently obtained. The IPCE values are lower limits as they are not corrected for the loss of light intensity caused by reflection by the quartz window. Such a high quantum efficiency of photon-to-electron conversion obtained by using a carotenoid as the sensitizer is very impressive, and was observed by us for the first time.

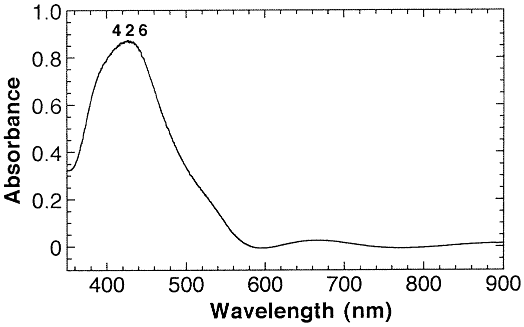

Fig. 5. Optical absorption spectrum of ACOA deposited on a piece of ITO/TiO_2 plate, versus bare ITO. The ITO/TiO_2 plate was immersed in ethanol solution of 0.3 mM ACOA for 4 h in dark at room temperature, and rinsed with clean ethanol three times before measurement.

Fig. 8 shows an open-circuit photovoltage response upon 426 nm monochromatic illumination (40 μW/cm^2) of ITO/TiO_2/ACOA electrode in a photoelectrochemical cell in several on-off cycles. The ITO/TiO_2/ACOA electrode showed negative polarity versus the Pt counter electrode. Photovoltage generation was instantaneous and rapidly reached a steady-state value of 150 mV. When the illumination was turned off, the photovoltage decayed back to zero

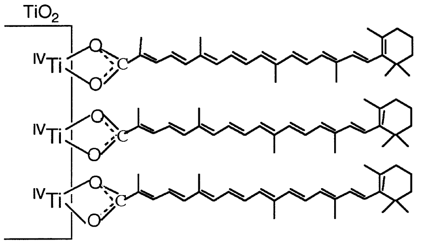

Scheme 3. Possible structure of ACOA complexes, probably forming an ordered monolayer, on the TiO_2 surface.

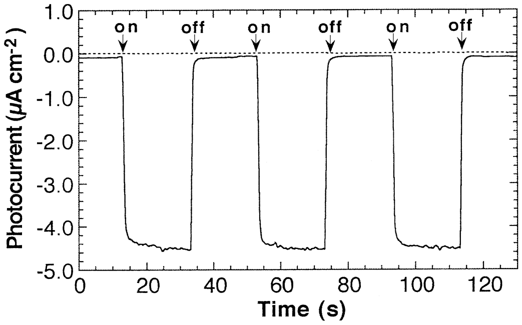

Fig. 6. Short-circuit photocurrent response of an ITO/TiO_2/ACOA electrode (solid line) and a bare ITO/TiO_2 plate (dotted line) in an electrochemical cell as the 426 nm monochromatic illumination (40 μW/cm^2) was turned on or off; aqueous 10 mM H_2Q and 0.1 M NaH_2PO_4 solution (pH = 7.4) pre-purged with argon for 20 min. The illuminated area is 0.25 cm^2; the counter electrode is a platinum flag (3.3 cm^2). The anodic current polarity is negative.

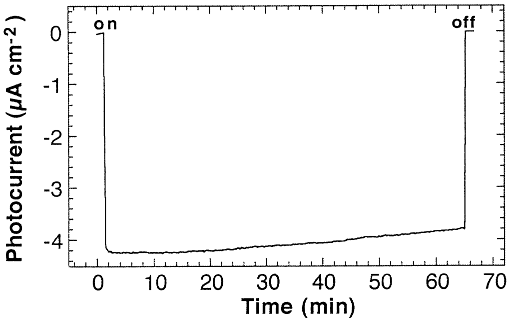

Fig. 7. Short-circuit photocurrent observed upon 1 h continuous 426 nm monochromatic illumination (40 μW/cm^2) of an ITO/TiO_2/ACOA electrode in an electrochemical cell. Other conditions were the same as in Fig. 6.

within seconds. Upon illumination, the photovoltage was very stable and remained at a constant value over hours.

3.5. Photocurrent action spectrum

A plot of the observed photocurrent (converted to IPCE value) as a function of the wavelength of the incident light upon illumination of the ITO/TiO_2/ACOA electrode in a photoelectrochemical cell is shown in Fig. 9.

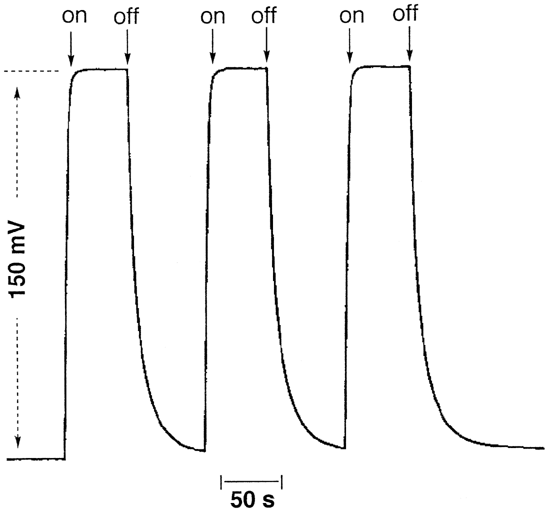

Fig. 8. Open-circuit photovoltage observed upon a few on/off cycles of 426 nm monochromatic illumination (40 μW/cm^2) of an ITO/TiO_2/ACOA electrode in an electrochemical cell. Other conditions were the same as in Fig. 6.

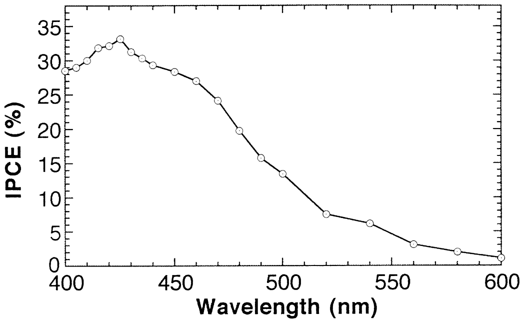

Fig. 9. Photocurrent action spectrum of an ITO/TiO_2/ACOA electrode in an electrochemical cell. Other conditions were the same as in Fig. 6. Cell operated in short-circuit mode.

The action spectrum closely resembles the absorption spectrum of ACOA layer deposited on the ITO/TiO_2 surface with the maximum IPCE value near 426 nm, therefore indicating that the observed photocurrents were indeed sensitized by ACOA deposited on ITO/TiO_2 electrode.

3.6. Photocurrent observed upon irradiation of ITO/TiO_2/ACOA electrode under applied bias

Fig. 10 shows the photocurrents observed upon 426 nm monochromatic illumination (70 μW/cm^2) of an ITO/TiO_2/ACOA electrode in a photoelectrochemical cell while the electrode was subjected to a bias of −0.15, 0, and +0.15 V (versus SCE). Under a bias of −0.15 V (the rest potential of the cell), the dark current was zero; the anodic photocurrent rose immediately upon illumination, and only slight decay was observed. Upon termination of illumination the photocurrent instantly returned to zero. The photocurrent increased as the potential of the working electrode was shifted to 0 V; in addition, a small dark anodic current appeared. This observation indicates that a positive bias facilitates electron transport across the TiO_2 nanocrystalline thin film toward

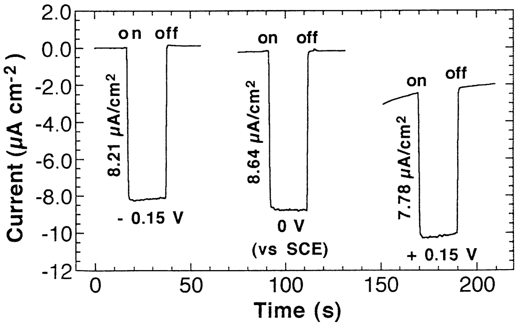

Fig. 10. Photocurrents observed upon 426 nm monochromatic illumination (70 μW/cm^2) of an ITO/TiO$_2$/ACOA electrode under applied bias of −0.15, 0, and +0.15 V versus SCE.

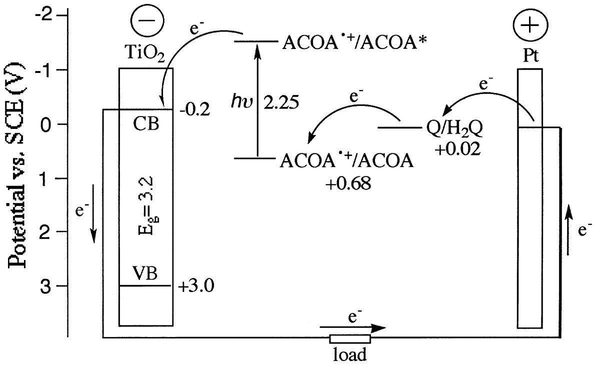

Scheme 4. Schematic representation of the carotenoid-sensitized TiO$_2$ photovoltaic response in the presence of electron donor H$_2$Q.

the ITO substrate. As the applied potential was shifted to a more positive bias of +0.15 V, however, suppression of the photocurrent was observed which is assumed to be due to the large increase of the dark current. The rapid growth of the anodic dark current as the applied potential was shifted to more positive bias arose from the direct oxidation of H$_2$Q (0.02 V versus SCE) at the exposed ITO on the working electrode.

3.7. Mechanism of photocurrent generation of carotenoid-sensitized TiO$_2$ electrode

Our results demonstrate that a photocurrent is indeed produced upon excitation of the carotenoid within the ITO/TiO$_2$/ACOA film followed by quenching of its excited state by electron injection into the TiO$_2$ conduction band, or by a carotenoid-sensitization process. Scheme 4 illustrates the proposed mechanism of this process and gives the relative locations of TiO$_2$, H$_2$Q, and the energy levels of the dye.

Upon illumination of the cell, the carotenoid ACOA molecules are electronically excited and inject electrons into the TiO$_2$ conduction band. These injected electrons traverse the TiO$_2$ film and are collected at the back contact (ITO electrode). After passing through the external circuit and delivering power to a load, the electrons re-enter the cell at the counter electrode, reduce the quinone to H$_2$Q (1,4-benzoquinone + 2H$^+$ + 2e$^-$ = H$_2$Q, 0.02 V versus SCE at pH 7.4 in aqueous solution), which then reduces the photo-oxidized carotenoid (ACOA$^{\bullet+}$) back to its original state. The fact that the photocurrent was nearly constant during 1 h of continuous illumination indicates that these carotenoids bound to TiO$_2$ are stable at the electrode/electrolyte interface, presumably because of rapid regeneration of ACOA from ACOA$^{\bullet+}$ by electron transfer from the electron donor H$_2$Q. The oxidation of H$_2$Q probably occurs by a single electron transfer to ACOA$^{\bullet+}$, followed by very rapid loss of a proton to yield HQ$^{\bullet}$, and two HQ$^{\bullet}$s react to form H$_2$Q and Q by a disproportionation step (Scheme 5).

$$H_2Q + ACOA^{\cdot+} = H_2Q^{\cdot+} + ACOA$$
$$H_2Q^{\cdot+} = HQ^{\cdot} + H^+$$
$$2HQ^{\cdot} = H_2Q + Q$$

Scheme 5.

From the difference between the potential levels of Q/H$_2$Q and the TiO$_2$ CB, the theoretical open-circuit voltage can be estimated as 0.22 V; it is very close to the experimental value 0.15 V considering energy losses in photoinjection, traverse, and collection processes in the cell. Proper choice of other redox relays with a potential level more positive than Q/H$_2$Q (but always more negative than that of ACOA$^{\bullet+}$/ACOA) could give the cell a higher open-circuit voltage. This aspect should be investigated in future studies.

Back reactions such as recombination of the injected electron with the oxidized form of the carotenoid (ACOA$^{\bullet+}$) or H$_2$Q$^{\bullet+}$ could occur and would reduce the cell efficiency. However, the high IPCE at maximum wavelength obtained in the discussed cell using ACOA as the photosensitizer indicates that the recombination process is slow. The rapid loss of a proton from H$_2$Q$^{\bullet+}$ to form HQ$^{\bullet}$ radical probably decreases possible electron transfer from the TiO$_2$ to H$_2$Q$^{\bullet+}$. It is known that in carotenoid radical cations *trans*/*cis* geometrical isomerization processes can occur [46]. Therefore, geometrical isomerization of ACOA molecules on the TiO$_2$ surface accompanying the electron transfer process might explain the slow electron recombination process of the injected electrons with ACOA$^{\bullet+}$. Photochemical *trans*/*cis* isomerization of carotenoids via triplet states can also occur [47]. It might be relevant to mention that in the visual system carotenoid 11-*cis*-retinal binds to an opsin protein to form the visual pigment rhodopsin in the eye; rhodopsin absorbs a photon of light, leading to the *cis* to *trans* isomerization of its protonated 11-*cis*-retinal Schiff base chromophore [48]. In addition, the carotenoid conjugated structure serving as ‘molecular wires’ or ‘electron mediators’ and having photoconduction properties in the TiO$_2$/ACOA film would facilitate the photoinjection and movement of electrons and therefore result in high cell efficiency.

4. Conclusions

We have demonstrated that photovoltaic currents are generated upon illumination of ITO electrodes coated with a TiO_2 nanocrystalline mesoporous membrane with the carotenoid 8′-apo-β-caroten-8′-oic acid (ACOA) as the sensitizer and immersed in an aqueous electrolyte solution containing hydroquinone (H_2Q). The short-circuit photocurrent reached 4.6 μA/cm^2 upon 426 monochromatic illumination at 40 μW/cm^2 with an IPCE of 34% and an open-circuit photovoltage of 0.15 V. The photocurrent and photovoltage were stable during 1 h continuous irradiation. The action spectrum indicates that the carotenoid-sensitization processes on the TiO_2 surface account for the generation of the photocurrent.

Acknowledgements

Dr. Elli Hand is thanked for synthesizing 8′-apo-β-caroten-8′-oic acid. This work was supported by the Division of Chemical Sciences, Office of Basic Energy Sciences, Office of Energy Research of the US Department of Energy under Grant No. DE-FG02-86-ER13465.

References

[1] M. Kuki, Y. Koyama, H. Nagae, J. Phys. Chem. 95 (1991) 7171.
[2] H. Hashimoto, Y. Miki, M. Kuki, T. Shimamura, H. Utsumi, Y. Koyama, J. Am. Chem. Soc. 115 (1993) 9216.
[3] R. Edge, D.J. McGarvey, T.G. Truscott, J. Photochem. Photobiol. B: Biology 41 (1997) 189.
[4] A. Slama-Schwok, M. Blanchard-Desce, J.-M. Lehn, J. Phys. Chem. 94 (1990) 3894.
[5] M.P. Debreczeny, M.R. Wasielewski, S. Shinoda, A. Osuka, J. Am. Chem. Soc. 119 (1997) 6407.
[6] D. Carbonera, M. di Valentin, C. Corvaja, G. Giacometti, G. Agostini, P.A. Liddell, A.L. Moore, T.A. Moore, D. Gust, J. Photochem. Photobiol. A: Chemistry 105 (1997) 329.
[7] P.A. Liddell, D. Kuciauskas, J.P. Sumida, B. Nash, D. Nguyen, A.L. Moore, T.A. Moore, D. Gust, J. Am. Chem. Soc. 119 (1997) 1400.
[8] A.S. Jeevarajan, L.D. Kispert, N.I. Avdievich, M.D.E. Forbes, M.J. Phys. Chem. 100 (1996) 669.
[9] T.A. Konovalova, L.D. Kispert, V.V. Konovalov, J. Phys. Chem. B 101 (1997) 7858.
[10] G. Gao, Y. Deng, L.D. Kispert, J. Phys. Chem. 102 (1998) 3897.
[11] H.T. Witt, Biochim. Biophys. Acta 505 (1979) 355.
[12] J.R. Platt, Science 129 (1959) 372.
[13] M. Calvin, Science 184 (1974) 375.
[14] B. Rosenberg, J. Chem. Phys. 31 (1959) 238.
[15] R.J. Cherry, D. Chapman, Mol. Cryst. 3 (1967) 251.
[16] R.J. Cherry, Quart. Rev. 22 (1968) 160.
[17] A. Diarra, S. Hotchandani, J.J. Max, R.M. Leblanc, J. Chem. Soc. Faraday Trans. 282 (1986) 2217.
[18] L. Sereno, J.J. Silber, L. Otero, M.del V. Bohorquez, A.L. Moore, T.A. Moore, D. Gust, J. Phys. Chem. 100 (1996) 814.
[19] A. Mills, S.L. Hunte, J. Photochem. Photobiol. A: Chem. 108 (1997) 1.
[20] A. Hagfeld, M. Graetzel, Chem. Rev. 95 (1995) 49.
[21] Dye Sensitization of Semiconductors, Workshop Report, organized by the National Renewable Energy Laboratory, sponsored by the U.S., Department of Energy, Office of Energy Research, Office of Basic Energy Sciences, Division of Chemical Sciences, 10–11 March 1997, Golden, Colorado.
[22] Abstracts in 12th International Conference on Photochemical Conversion and Storage of Solar Energy, 9–14 August 1998, Berlin, Germany.
[23] E. Borgarello, J. Kiwi, E. Pelizetti, M. Visca, M. Graetzel, J. Am. Chem. Soc. 103 (1983) 6423.
[24] D.N. Furlong, D. Wells, W.H.F. Sasse, J. Phys. Chem. 90 (1986) 1107.
[25] P.V. Kamat, M.A. Fox, Chem. Phys. Lett. 102 (1983) 379.
[26] J. Moser, M. Graetzel, J. Am. Chem. Soc. 106 (1984) 6557.
[27] A. Giraudean, F.R.F. Fan, A.J. Bard, J. Am. Chem. Soc. 102 (1980) 5137.
[28] D. Liu, P.V. Kamat, J. Electrochem. Soc. 142 (1995) 835.
[29] C.Y. Wang, C.Y. Liu, W.Q. Wang, T. Shen, J. Photochem. Photobiol. A: Chem. 109 (1997) 159.
[30] G. Gao, Y. Deng, L.D. Kispert, J. Chem. Soc. Perkin Trans. 2 6 (1999) 1225.
[31] Elli Hand, to be published elsewhere.
[32] B. O'Regan, J. Moser, M. Anderson, M. Graetzel, J. Phys. Chem. 94 (1990) 8720.
[33] B. O'Regan, M. Graetzel, Nature 353 (1991) 737.
[34] M. Khaled, A. Hadjipetrou, L.D. Kispert, J. Phys. Chem. 94 (1990) 5164.
[35] M. Khaled, A. Hadjipetrou, L.D. Kispert, J. Phys. Chem. 95 (1991) 2438.
[36] A.S. Jeevarajan, M. Khaled, L.D. Kispert, J. Phys. Chem. 98 (1994) 7777.
[37] A.S. Jeevarajan, M. Khaled, L.D. Kispert, Chem. Phys. Lett. 225 (1994) 340.
[38] J.A. Jeevarajan, L.D. Kispert, J. Electroanal. Chem. 411 (1996) 57.
[39] J.A. Jeevarajan, A.S. Jeevarajan, L.D. Kispert, J. Chem. Soc. Faraday Trans. 92 (1996) 1757.
[40] Y. Paz, Z. Luo, L. Rabenberg, A. Heller, J. Mater. Chem. 10 (1995) 2482.
[41] A.J. Nozik, in: Dand El-Akabi H. Ollis (Eds.), Photocatalytic Purification and Treatment of Water and Air, Elsevier, New York, 1993, p. 39.
[42] S. Tunesi, M.A. Anderson, Langmuir 8 (1992) 487.
[43] S.J. Hug, B. Sulzberger, Langmuir 10 (1994) 3587.
[44] T. Rajh, A.E. Ostafin, D.M. Tiede, M.C. Thurnauer, 0.1. Micic, J. Phys. Chem. 100 (1996) 4538.
[45] P.V. Kamat, I. Bedja, S. Hotchandani, L.K. Patterson, J. Phys. Chem. 100 (1996) 4900.
[46] G. Gao, C.C. Wei, A.S. Jeevarajan, L.D. Kispert, J. Phys. Chem. 100 (1996) 5632.
[47] H. Hashimoto, Y. Miki, M. Kuki, T. Shimamura, H. Utsumi, Y. Koyama, J. Am. Chem. Soc. 115 (1993) 9216.
[48] R.R. Rando, Angew. Chem. Int. Ed. Engl. 29 (1990) 461.